Research Article

Journal of Environmental Nanotechnology

Insights on pH-dependent Physicochemical Properties and Supercapacitance Ability of α-MoO_3

P. Janardhanan[1], Varuna Jayachandran[1], M. Elango[1*] and J. Manikandan[2]

[1]Department of Physics, PSG College of Arts and Science, Coimbatore, TN, India

[2]Department of Chemistry, PSG College of Arts and Science, Coimbatore, TN, India

Received: 14.07.2024 Accepted: 09.09.2024 Published: 30.09.2024

*elango@psgcas.ac.in

ABSTRACT

The transition towards supercapacitors for efficient energy storage provides a dynamic outcome for the global warming. The MoO_3 samples were prepared at various pH using facile wet-chemical approach. The orthorhombic phase (α-MoO_3) was confirmed from structural investigations namely XRD, and Raman. It is also evident that the prepared samples show layered structure of MoO_3, which contributed in improving the efficiency of the supercapacitor application. The morphological analysis from SEM micrographs showed a slight agglomeration. The cyclic voltammetric studies revealed that the sample prepared at pH-10 displayed a higher specific capacitance.

Keywords: α-MoO_3; Wet-chemical; Microstructure; Electrochemical properties; Electric double layer capacitor.

1. INTRODUCTION

A strong demand for a shift towards renewable and sustainable energy is the essential solution for addressing the alarming global warming and climate change. For electricity and transportation, the reliance on fossil fuel increases greenhouse gas production and intensifies the environmental challenges. Therefore, implementing renewable energy resources create promising sustainable future, where energy production and environmental preservation are in harmony by curbing greenhouse gas emissions (Mensah-Darkwa *et al*. 2019). Supercapacitors play a significant role in replacing batteries in hybrid electric vehicles and portable electronic devices with many interesting properties namely, high power output, prolonged operational lifespans, rapid cycling rates, remarkable stability, and durability. Supercapacitors made of inorganic materials show superior structural, electrical, storage properties along with a non-toxic nature, cost effective and eco- friendly (Thillaikkarasi and Ramesh, 2022). The various inorganic materials being researched like Fe_2O_3, CuO, NiO, and MnO_2 have gained a huge attention due to their lightweight architecture (Shao *et al*. 2021; El-Nady et al. 2022; Yue et al. 2022). Among them, MoO_3 has unique structural properties with a potential role towards sensors, hydrogen storage, piezoelectric devices, electrocatalysts, batteries and supercapacitors. It is an n-type semiconductor with an energy gap of ≥ 3 eV (Kodan *et al*. 2018).

MoO_3 possesses three distinct polymorphs namely stable (α-MoO_3) orthorhombic, metastable (β-MoO_3) monoclinic, and (h-MoO_3) hexagonal. The phase of α-MoO_3 consists of double-layered [MoO_6] octahedral units. The β-MoO_3 displays a three-dimensional structure in which the corner oxygen atoms are shared by [MoO_6] octahedra. The h-MoO_3 has a one-dimensional tunnel-like structure comprising a zigzag chain of [MoO_6] octahedra. Among these phases, α-MoO_3 is specifically well-suited for charge storage owing to its distinct layered structure parallel to the (010) direction, which provides open channels that enable the intercalation at various sites (Chithambararaj *et al*. 2016). The thermodynamically stable and 2D layered orthorhombic phase (α) of MoO_3 can be prepared by a simple precipitation approach with appreciable mechanical stability and specific capacitance. An appreciable specific capacitance value of around 240 F g^{-1} was reported at a current density of 1.5 mA cm^{-2}. A capacitance retention of 78.8% even after 5000 cycles was achieved by 2D α-MoO_3 nanosheets synthesized *via* magnetron sputtering (Murugesan *et al*. 2019). Novel structure of MoO_3/MoO_3 /SiO_2 prepared *via* electrodeposition shows the power density of about 1000 W Kg^{-1} and with an energy density of 78 Wh Kg^{-1} with around 98% cyclic stability over 8000 cycles, whereas, poly dispersed MoO_3 displayed a specific capacitance of 835 F g^{-1} at 1 A g^{-1}. In another current research, α-MoO_3 were prepared through a simple wet chemical route and calcined at 500 °C (Zhao *et al*. 2020). The structural, morphological, optical, and capacitance properties of the samples were studied. The electrochemical

supercapacitance of the sample was tested for 1 M KOH as the electrolyte.

2. MATERIALS AND METHODS

2.1 Materials

The analytical grade precursor chemicals namely ammonium molybdate tetrahydrate [$(NH_4)_6Mo_7O_{24}.4H_2O$], nitric acid, liquid ammonia were purchased from Merck, India. All the chemicals were used without any further purification process.

2.2 Preparation Protocol

The MoO_3 samples at different pH were prepared by employing facile wet-chemical approach. Typically, 0.2 mol of molybdate precursor was dissolved in 100 mL of deionized water and subjected to constant stirring for 30 mins. After complete dissolution, 25 mL of concentrated HNO_3 was added in drops to the solution. The homogeneous mixture underwent a constant stirring at 85 °C for 3 hours, followed by the addition of liquid ammonia (precipitating agent) to the solution until pH-9 was attained. After that, the precipitate was aged at room temperature for about 4 hours. The collected precipitate was centrifuged at 3000 rpm for 10 mins and rinsed thoroughly several times with acetone and ethanol to remove the impurities. Then, the precipitate after washing was dried at 120 °C for 24 hours. Later, the dried precipitate was calcined at 500 °C for 3 hours. The MoO_3 sample prepared at pH-9 was collected and stored for characterization.

The aforementioned protocol was repeated for pH-10 and pH-11 as well. Finally, the samples prepared at different pH (9.0, 10.0, and 11.0) were analyzed for structural optical and super capacitance properties.

3. SAMPLE CHARACTERIZATION

The structural and morphological characterization techniques used include XRD, Raman spectroscopy, and SEM. A three-electrode system was employed for recording the electrochemical activity of the samples with KOH as electrolyte.

4. RESULTS AND DISCUSSIONS

4.1 X-ray Diffraction

Fig. 1 presents the X-ray diffraction spectra of the as prepared samples and it form a basis for investigating the crystalline nature and phase purity of the samples. The MoO_3 samples prepared at different pH values exhibited orthorhombic crystal structure. The sharp and well-defined peaks indicate the multi-faceted growth. The observed peaks at around ~12.8°, 23.1°, 25.7°, 27.2°, 29.6°, 33.8°, 35.5°, 38.9°, 46.1°, and 49.4° correspond to the Miller planes (020), (110), (040), (021), (130), (111), (041), (060), (210), and (002), respectively. The absence of parasitic phase shows the phase purity of the samples prepared and the results accord well with the JCPDS card 05-0508 (space group - Pbnm (62)) (M. Shashank *et al*., 2021). It is prominently evident that the planes (110), (040), and (021) at 23.1°, 25.7°, 27.2° respectively confirm stable orthorhombic (α-MoO_3) phase that is thermodynamically stable. The unit cell parameters were calculated to be a = 3.955 nm, b = 13.84 nm and c =3.69 nm (matched with ICDD card No.: 00-05-0508). The high-intense peaks imply the formation of layered structured of α -MoO_3 unit cells in anisotropic way (Usha *et al*. 2023). From the observed XRD spectra, d spacing, crystallite size, micro-strain, and other crystallographic parameters were found. The microstructural attributes of the samples (Table 1) were calculated using the following relations.

$$n\lambda = 2d \sin\theta \quad \ldots (1)$$

$$D = (K\lambda)/(\beta \cos\theta) \quad \ldots (2)$$

$$\varepsilon = (\beta \cos\theta)/4 \quad \ldots (3),$$

where n is the order of reflection (n=1), d is the interplanar spacing (nm), θ be the Bragg's diffraction angle, D indicates crystallite size obtained from the Debye-Scherrer formula, β is the full width at half maxima, ε denotes micro-strain. The texture coefficient of (110) and (040) was lesser than (021) plane. The higher TC_{hkl} of (021) attributes the better orientation due to insufficient interfacial energy, which eventually accelerates the nucleation and coalescence resulting in preferential orientation of the atoms in the specific direction (021) (Prakash *et al*. 2018).

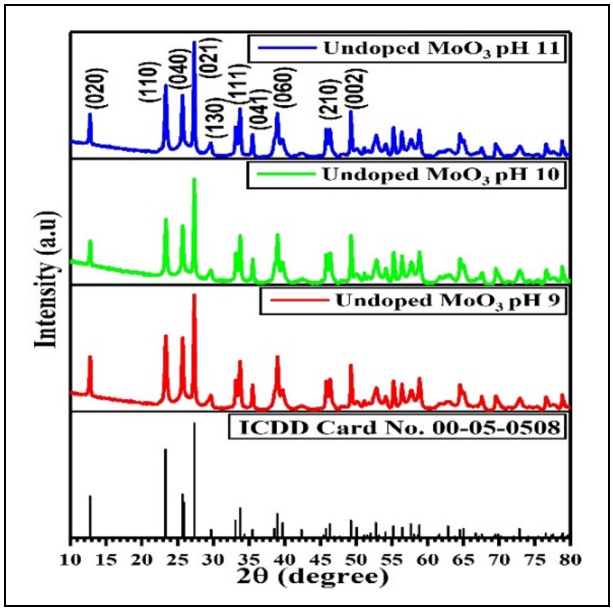


Fig. 1: XRD spectra of undoped MoO_3 nanoparticles at pH 9, pH 10 and pH 11

Table. 1 Microstructural property of MoO_3 nanoparticles at pH 9, pH 10 and pH 11

Samples	Crystallite Size (nm)	Micro Strain ($\times 10^{-3}$)
pH-9.0	48	0.0069
pH-10.0	45	0.0066
pH-11.0	46	0.0061

4.2 Raman Spectra

The vibrational spectra were recorded using a Raman laser excitation line to investigate the bonding nature and local structure of the prepared samples (Fig. 2). This effective tool provides information about the forces raised from mutual interactions of electrons and nuclei. The bands obtained from the spectra are assigned using Py - Masche model (Py and Maschke 1981). The characteristic Raman bands 670, 822, and 1000 cm^{-1} attribute the layered configuration of orthorhombic MoO_3 structure. The 670 cm^{-1} can be assigned to the symmetric stretching mode of triply coordinated bridge oxygen (Mo3-O: B_{2g}, B_{3g}) atoms originating from sharing of oxygen located at the corner of the crystallites. The Raman bands around 822 and 1000 cm^{-1} are symmetric ($Mo^{2-}O$: A_g, B_{1g}) and asymmetric (Mo^{6+}=O: A_g, B_{1g}) stretching modes of doubly coordinated oxygen and unshared oxygen atoms, respectively (Shahsank *et al*. 2021) The bands at 340 and 385 cm^{-1} can be related to the scissoring (B_{3g}) and wagging (B_{1g}) modes of O – Mo – O. The twisting and wagging modes of double bond O = Mo = O appeared around 244 (B_{3g}) and 294 (B_{2g}) cm^{-1}, respectively. From the observed Raman spectra, it is evident that the prepared samples are orthorhombic in phase and it conforms well with the XRD findings.

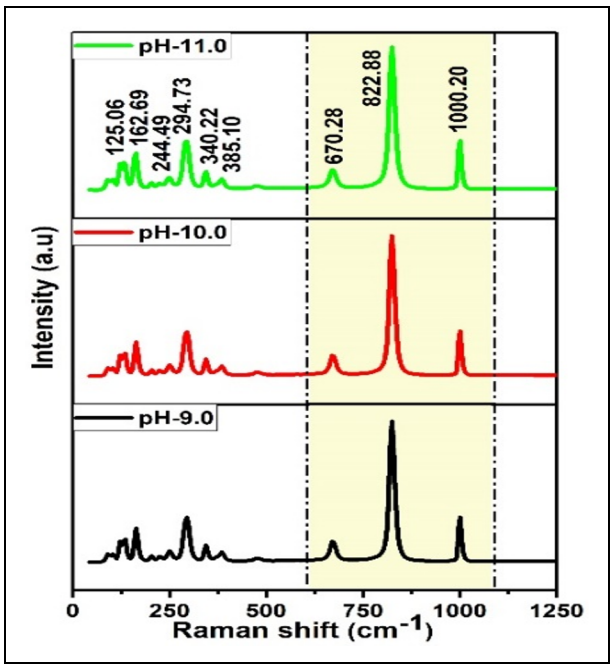


Fig. 2: Raman Spectra of undoped MoO_3 nanoparticles at pH 9, pH 10 and pH 11

4.3 SEM Analysis

The SEM micrographs of MoO_3 prepared at pH-10.0 is presented in Fig. 3. The SEM micrographs show non-uniform mere spherical morphology with sparse agglomeration. The high surface energy stabilization might be the cause of the agglomeration. This was achieved via Ostwald's ripening process during growth of crystallites reaction (Lou and Zeng 2002). The particle size distribution calculated from the obtained micrograph was ~ 20 nm. From the FESEM analysis, it was realized that the individual particle boundaries in spite of particle agglomeration occur. During the synthesis no surfactant was used in any form of in order to prevent particle aggregation. This resulted in mild agglomeration of particles.

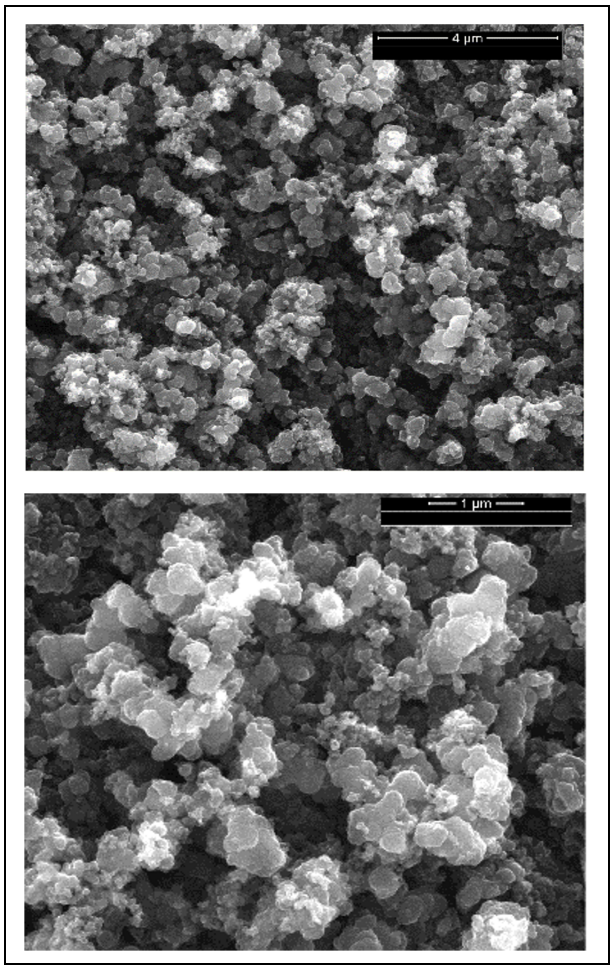


Fig. 3: SEM micrograph of undoped MoO_3 nanoparticles at pH 10

4.4 CV Studies

The CV study of the prepared MoO_3 samples were recorded using a reference, working, auxiliary electrode workstation at various scan rates (10, 20, 30, 40, and 50 mV/s) in a potential window of -500 to 500 mV and are shown in Fig 4. The electrolyte of 1 M KOH

was employed to study the electrochemical activity. The CV graphs display the redox cycles of Faradaic reactions similar to electric double layer capacitor (EDLC). The specific capacitance of the MoO_3 synthesized at pH-9, 10, and 11 are 420, 460, and 333 F g^{-1}. Among them, MoO_3 synthesized at pH-10 at a scan rate 10 mV/s exhibited the highest specific capacitance.

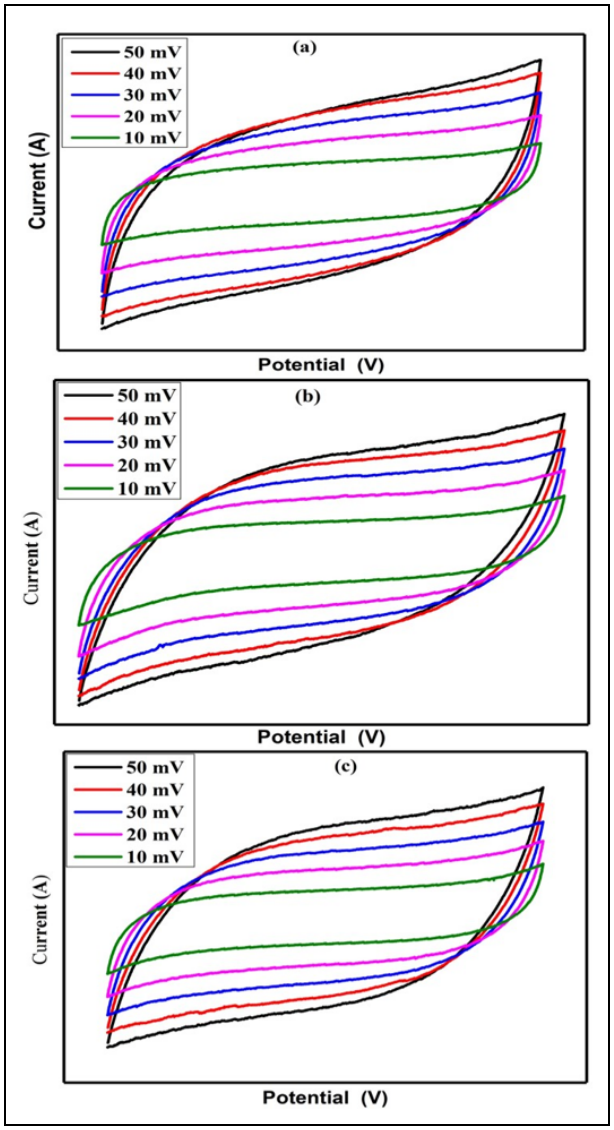


Fig. 4: Cyclic voltammetry analysis of undoped MoO_3 nanoparticles at pH 9 (a), pH 10(b) and pH 11(c)

5. CONCLUSION

The orthorhombic phase (α) MoO_3 were prepared at varying pH via simple co-precipitation method. The structural and morphological nature were analyzed through X-Ray diffraction, Confocal - RAMAN and Surface Emission Microscopy. The phase purity and multi-faceted growth were confirmed from the XRD and Raman. The layered structure of MoO_3 evidenced from the structural analysis are responsible for the witnessed electrochemical activity. The sparse agglomeration of non-uniform mere spherical morphology was revealed from FESEM analysis. The pH-10 prepared MoO_3 exhibited the high specific capacitance.

FUNDING

This research received no specific grant from any funding agency in the public, commercial, or not-for-profit sectors.

CONFLICTS OF INTEREST

The authors declare that there is no conflict of interest.

COPYRIGHT

This article is an open-access article distributed under the terms and conditions of the Creative Commons Attribution (CC BY) license (http://creativecommons.org/licenses/by/4.0/).

REFERENCES

Chithambararaj, A., Rajeswari Yogamalar, N. and Bose, A. C., Hydrothermally Synthesized h-MoO_3 and α-MoO_3 Nanocrystals: New Findings on Crystal-Structure-Dependent Charge Transport, *Cryst. Growth Des.*, 16(4), 1984–1995 (2016). https://doi.org/10.1021/acs.cgd.5b01571

Thillaikkarasi, D. and Ramesh, R., Synergetic Effect on Electrochemical Performance of Activated Carbon - Multiwalled Carbon Nanotubes Supercapacitor using various Electrodes in Aqueous Electrolyte, *J. Environ. Nanotechnol.,* 11(2), 04-21 (2022). https://doi.org/10.13074/jent.2022.06.222453

El-Nady, J., Shokry, A., Khalil, M., Ebrahim, S., Elshaer, A. M. and Anas, M., One-step electrodeposition of a polypyrrole/NiO nanocomposite as a supercapacitor electrode. *Sci. Rep.*, *12*(1), 3611 (2022). https://doi.org/10.1038/s41598-022-07483-y

Kodan, N., Singh, A. P., Vandichel, M., Wickman, B. and Mehta, B. R., Favourable band edge alignment and increased visible light absorption in β-MoO_3/α-MoO_3 oxide heterojunction for enhanced photoelectrochemical performance, *Int. J. Hydrogen Energy*, 43(33), 15773–15783 (2018). https://doi.org/10.1016/j.ijhydene.2018.06.138

Lou, X. W. and Zeng, H. C., Hydrothermal Synthesis of α-MoO 3 Nanorods via Acidification of Ammonium Heptamolybdate Tetrahydrate, *Chem. Mater.*, 14 (11), 4781–4789 (2002). https://doi.org/10.1021/cm0206237

Mensah-Darkwa, K., Zequine, C., Kahol, P. K. and Gupta, R. K., Supercapacitor Energy Storage Device Using Biowastes: A Sustainable Approach to Green Energy, *Sustainability*, 11(2), 414 (2019). https://doi.org/10.3390/su11020414

Murugesan, D., Prakash, S., Ponpandian, N., Manisankar, P. and Viswanathan, C., Two dimensional α-MoO_3 nanosheets decorated carbon cloth electrodes for high-performance supercapacitors, *Colloids Surf A Physicochem Eng. Asp.*, 569, 137–144 (2019). https://doi.org/10.1016/j.colsurfa.2019.02.062

Prakash, N. G., Dhananjaya, M., Narayana, A. L., Shaik, D. P., Rosaiah, P. and Hussain, O.M., High Performance One Dimensional α-MoO3 Nanorods for Supercapacitor Applications, *Ceram. Int.*, 44 (8), 9967–9975 (2018). https://doi.org/10.1016/j.ceramint.2018.03.032

Py, M. A. and Maschke, K., Intra- and interlayer contributions to the lattice vibrations in MoO3, *Physica B+C*, 105(1–3), 370–374 (1981). https://doi.org/10.1016/0378-4363(81)90278-3

Shahsank, M., Bhojya Naik, H. S., Sumedha, H. N. and Nagaraju, G., Implementing an in-situ carbon formation of MoO_3 nanoparticles for high performance lithium-ion battery, *Ceram Int*, 47 (7), 10261–10267 (2021). https://doi.org/10.1016/j.ceramint.2020.07.241

Shao, W., Li, M., Wang, X., Fu, N. and Yang, Z., High-performance cobalt-doped carbon cloth supported porous Fe_2O_3 flexible electrode material in quasi-solid asymmetric supercapacitors, *J. Alloys Compd*, *929*, 167141 (2022). https://doi.org/10.1016/j.jallcom.2022.167141

Usha, T., Ranjith Kumar, E., Kumar, M., Balraj, B., Sivakumar, C., Matheswaran, P., Chandrasekar, N. and Kumar Nagarajan, S., Physicochemical properties and photocatalytic activity of MoO3 nanostructures: Evaluation of structural, optical, vibrational, and morphological properties, *Ceram Int*, 49(9), 13994–14006 (2023). https://doi.org/10.1016/j.ceramint.2022.12.281

Yue, T., Shen, B. and Gao, P., Carbon material/MnO_2 as conductive skeleton for supercapacitor electrode material: A review. *Renew. Sustain. Energy Rev. 158*, 112131 (2022). https://doi.org/10.1016/j.rser.2022.112131

Zhao, N., Fan, H., Zhang, M., Ma, J., Du, Z., Yan, B., Li, H. and Jiang, X., Simple electrodeposition of MoO3 film on carbon cloth for high-performance aqueous symmetric supercapacitors, *Chem. Eng. J.*, 390, 124477 (2020). https://doi.org/10.1016/j.cej.2020.124477